

## ARTICLE

## Climatology and Water Management

# Evaluation of DSSAT-MANIHOT-Cassava model to determine potential irrigation benefits for cassava in Jamaica

Dale Rankine<sup>1</sup>  | Jane Cohen<sup>2</sup>  | Fradian Murray<sup>2</sup> | Patricia Moreno-Cadena<sup>3,4,5</sup>  | Gerrit Hoogenboom<sup>3,6</sup>  | Jayaka Campbell<sup>1</sup> | Michael Taylor<sup>1</sup> | Tannecia Stephenson<sup>1</sup>

<sup>1</sup> Dep. of Physics, Univ. of the West Indies, Kingston 7, Mona, Jamaica

<sup>2</sup> Dep. of Life Sciences, Univ. of the West Indies, Kingston 7, Mona, Jamaica

<sup>3</sup> Agricultural and Biological Engineering Dep., Univ. of Florida, Frazier Rogers Hall, PO Box 110570, Gainesville, FL 32611-0570, USA

<sup>4</sup> Alliance of Bioversity International and International Center for Tropical Agriculture (CIAT), km 17 recta Cali–Palмира, Cali 763537, Colombia

<sup>5</sup> International Institute of Tropical Agriculture (IITA), ICIPE Campus, Nairobi P.O. Box 30772-00100, Kenya

<sup>6</sup> Institute for Sustainable Food Systems, Univ. of Florida, Frazier Rogers Hall, PO Box 110570, Gainesville, FL 32611-0570, USA

## Correspondence

Dale Rankine, Dep. of Physics, Univ. of the West Indies, Mona, Kingston 7, Jamaica.  
Email: [rankinedr@gmail.com](mailto:rankinedr@gmail.com)

Assigned to Associate Editor Stephen Del Grosso.

## Funding information

Adaptation Programme and Financing Mechanism of the National Pilot Programme for Climate Resilience, Grant/Award Number: EFJ94102968

## Abstract

Cassava (*Manihot esculenta* Crantz) is an important food crop, especially in developing countries, because of its resilience and ability to grow in conditions generally inhospitable for other crops. However, tropical crops like cassava are not as frequently modeled compared with crops from temperate locations. The objective of this research was to calibrate the CSM-MANIHOT-Cassava model of the Decision Support System for Agrotechnology Transfer, DSSAT beta v4.8 and use the model to evaluate the potential benefits of irrigation on yield. We established two field trials with two water treatments (rainfed and irrigated) and four cultivars that had not been studied previously. We simulated in-season biomass and end-of-season yield, evaluating the model performance with different statistical measures. There was good agreement between simulated and measured values; the best results showed a deviation of 9.7%, normalized RMSE of 18%, and *d*-index of 0.98 for biomass, with corresponding values of 11, 24, and 0.98, respectively, for yield. Good simulations of yield correlated with accurate simulations for leaf area index and harvest index. The varieties showed differential responses to irrigation, suggesting that there are diverse levels of drought tolerance even within the same environmental conditions.

**Abbreviations:** CSM, Cropping System Model;; DAP, days after planting; DSSAT, Decision Support System for Agrotechnonology Transfer; HI, harvest index; LAI, leaf area index; LLIFA, leaf life from full expansion to start of senescence; LNSLP, slope for leaf production; LPEFR, leaf petiole fraction; PAR, photosynthetically active radiation; RAW, readily available water; RSME<sub>n</sub>, normalized root mean square error; WUE, water use efficiency.

This is an open access article under the terms of the [Creative Commons Attribution-NonCommercial-NoDerivs](https://creativecommons.org/licenses/by-nc-nd/4.0/) License, which permits use and distribution in any medium, provided the original work is properly cited, the use is non-commercial and no modifications or adaptations are made.

© 2021 The Authors. *Agronomy Journal* published by Wiley Periodicals LLC on behalf of American Society of Agronomy

The model was able to simulate total crop failure in harsh drought conditions, suggesting it can be used as a key decision-making tool in unfavorable conditions that will be occasioned by climate change.

## 1 | INTRODUCTION

Cassava (*Manihot esculenta* Crantz) is a perennial shrub belonging to the dicotyledonous family Euphorbiaceae that is primarily cultivated for its starchy roots, although its leaves and stems are also useful (Alves, 2002; CIAT, 2011; El-Sharkaway, 2004; Mtunguja et al., 2016). In global production of roots and tubers, cassava is ranked second to potato (*Solanum tuberosum* L.), and its increasing production is contrasted to the relative decline of that of potato (FAO, 2020). The crop is cultivated in most tropical countries located between 30° N and 30° S for food, feed, and biofuel production (Ayling et al., 2012; Gabriel et al., 2014; Prochnik et al., 2012). In Jamaica, cassava is among the top three root crops. Cassava is prepared in many ways for human consumption, including boiled, baked, fried. It is also used to make gluten-free flour and, more recently, in beer as a substitute for high-maltose corn syrup.

Cassava is regarded as a versatile and resilient crop that can grow under conditions that are usually inhospitable to the cultivation of other crops. It grows in areas with poor soils (Alves, 2002; CIAT, 2011), is tolerant to drought (Alves, 2002; El-Sharkawy, 2004), and is efficient at transforming solar energy to carbohydrate (Tonukari, 2004). Traditionally, cassava cultivation is rainfed without supplemental irrigation and grows with as little as 400 mm of annual rainfall. However, the crop requires about 50–100 mm of water for good germination (Isaiah et al., 2020). Yield increases with higher water availability, and the FAO regards 1,000–1,500 mm as the optimal range for rainfall for cassava cultivation (FAO, 2013a).

Climate change poses several risks to the agricultural sector in Jamaica as well as the wider Caribbean. Temperatures in the Caribbean have been increasing, and rainfall has exhibited marked interannual variability. As a result, there has been an increase in the frequency of severe weather events, and sea levels have risen (Climate Studies Group Mona [CSGM], 2012, 2017; Stephenson et al., 2014). Climate models suggest conditions will be more challenging, with projections that coalesce around warmer (by between 1 and 4 °C) and drier conditions (up to 40%), with even higher sea levels and more intense severe weather events as mid-century and the end of the century are approached (CSGM, 2017). With the increasing effects of climate change on food security, East Africa has made significant efforts to increase cassava production, among other drought-tolerant species such as sorghum [*Sorghum bicolor* (L.) Moench] and pearl millet

[*Pennisetum glaucum* (L.) R. Br.] (Reincke et al., 2018). It is predicted that by 2050 there will be increased consumption of root and tuber crops compared with 2010 by at least 8% in developing countries (Scott, 2021). Similar concerns exist in the Caribbean, and efforts are underway to promote the consumption of locally produced, healthier foods, reducing reliance on more expensive and imported alternatives (FAO, 2013b; Robin et al., 2018).

Investigating the limits of cassava's resilience to climate change and identifying cultivars that should be prioritized would be both time and cost prohibitive if done using only experimental field methods. Crop models are helpful for testing and evaluating field studies and experimenting with new management options (Tsuji et al., 1998). In this regard, crop simulation modeling can provide key advantages, but this is one area that has not been well explored in the Caribbean, primarily due to a lack of models that have been evaluated for local conditions and the focus of research on other areas, including postharvest losses (Brockamp, 2016; FAO, 2015), value-chain development (Robin et al., 2018), and food and nutrition security (FAO, 2013b).

Eighteen crop models have been developed for cassava (Moreno-Cadena et al., 2021). Listed among these are the following models: the Simple and Universal CROp growth Simulation Model (SUCROS) (Penning de Vries & Laar, 1982; Gijzen et al., 1990), the Light Interception and Utilization Model (LINTUL) (Adiele et al., 2021; Ezui et al., 2018), GUMCAS (Matthews & Hunt, 1994), Cropping System Model (CSM)-CROPSIM (Hoogenboom, Porter, Boote, et al., 2019; Hoogenboom, Porter, Shelia, et al., 2019), and CSM-MANIHOT (Hoogenboom, Porter, Boote, et al., 2019; Hoogenboom, Porter, Shelia, et al., 2019; Moreno-Cadena, 2018; Moreno-Cadena et al., 2020). The SUCROS model simulates plant growth based on total photosynthesis and accounts for respiration losses. The allocation of assimilates to different plant organs varies with development stage and tuber growth (Moreno-Cadena et al., 2021). However, the model was calibrated using data from one location (Colombia), which limits its application to other regions (Moreno-Cadena et al., 2021; Veltkamp, 1986). The LINTUL cassava model (Ezui et al., 2018) was developed to investigate cassava growth and yield under water-limiting conditions and with different planting dates in rainfed systems in West Africa (Adiele et al., 2021; Moreno-Cadena et al., 2021). The model represented an improvement to the SUCROS model because its simulations were based on intercepted

radiation more than on the trade-off between photosynthesis and respiration (Moreno-Cadena et al., 2021).

The GUMCAS model was developed for use in the International Benchmark Sites Network for Agrotechnology Transfer decision support system to describe cassava growth and the effect of water stress on various developmental stages of the crop (Matthews & Hunt, 1994). The model has three distinct growth phases: (a) planting to emergence, (b) emergence to first branching, and (c) first branching to harvest maturity (Moreno-Cadena et al., 2021). The GUMCAS model was the first to incorporate vapor pressure deficit effects on stomatal conductance and modified growth rates under drought stress. Although GUMCAS is an improvement over previous models, it is not ideally suited for accurate cassava simulation because the crop does not have distinct growth phases. Moreover, unlike the assumptions of GUMCAS, branching rates are not constant after the occurrence of the first branching. The CSM-CROPSIM model was developed from the GUMCAS model for use in the Decision Support System for Agrotechnology Transfer (DSSAT) but has undergone some critical modifications. It uses air temperature and not soil temperature for estimating germination and emergence. The development rate is not modified for drought stress, and there are improvements to the effects of photoperiod, fibrous, and storage root growth (Moreno-Cadena et al., 2021). The model uses 10 ecotype parameters and 21 cultivar-specific parameters. A comprehensive review of these cassava models is given in Moreno-Cadena et al. (2021). The CSM-MANIHOT-Cassava model (referred to as MANIHOT-Cassava in the remainder of the paper) was developed as an improved version of the CSM-CROPSIM. It contains new processes that more accurately represent the growth of stems, leaves, and branches and improves biomass and yield simulations (Moreno-Cadena et al., 2020; Phoncharoen, Banterng, Moreno-Cadena, et al., 2021). MANIHOT-Cassava (DSSAT beta v4.8, 2021) uses 15 ecotype and only 15 cultivar-specific parameters (Hoogenboom, Porter, Boote, et al., 2019; Hoogenboom, Porter, Shelia, et al., 2019; Hoogenboom et al., 2021; Moreno-Cadena et al., 2020, 2021). It can be applied to varying environmental conditions and management systems and is considered the default cassava model of the DSSAT crop modeling ecosystem (Hoogenboom, Porter, Boote, et al., 2019; Moreno-Cadena et al., 2020; Phoncharoen, Banterng, Moreno-Cadena, et al., 2021). The model has been used to identify potential cassava genotypes for different production systems in Thailand (Phoncharoen, Banterng, Vorasoot, et al., 2021) and to investigate the sensitivity of parameters to yield in Colombia (Moreno-Cadena et al., 2020). Given its ease of access, applicability to different regions, and improved accuracy, we chose the MANIHOT-Cassava model for this study. Furthermore, MANIHOT-Cassava has not been previously evaluated for Jamaica and the wider Caribbean, and in this context, this work stands to make an original contribution.

### Core Ideas

- The study calibrated four cassava cultivars in the CSM-MANIHOT-Cassava model.
- The model can simulate crop failure under high drought stress conditions.
- With climate change, irrigation is critical for future production of cassava in Jamaica.
- The model can be used to prioritize climate change adaptation options for agriculture.

The first objective of this study was to calibrate MANIHOT-Cassava in DSSAT Beta v4.8 (2021) (Hoogenboom, Porter, Boote, et al., 2019; Hoogenboom, Porter, Shelia, et al., 2019; Hoogenboom et al., 2021; Jones et al., 2003) within a small island developing state context. In addition, it would represent the first work with the latest version (DSSAT v4.8 2021) of MANIHOT-Cassava. We predicted the yield and biomass of four locally grown cassava genotypes in rainfed and irrigated conditions. The Caribbean region faces a number of challenges with respect to climate change. Given the over-reliance on rainfed agriculture, the projections for warmer and drier conditions bear serious implications for agriculture. The second objective of this study was to investigate the potential benefits of irrigation using different irrigation thresholds of the model. Considering the projections for drier weather, this study could give helpful insights into future water requirements for viable production.

## 2 | MATERIALS AND METHODS

### 2.1 | Description of the CSM-MANIHOT-Cassava model

The MANIHOT-Cassava model (version 4.8.0.006) is part of the DSSAT Beta V4.8 family of models (Hoogenboom, Porter, Boote, et al., 2019; Hoogenboom, Porter, Shelia, et al., 2019; Hoogenboom et al., 2021; Moreno-Cadena, 2018; Moreno-Cadena et al., 2020, 2021). It simulates growth and development, providing details of the pathways taken from sowing to final harvest, and in this regard is termed a dynamic crop model. It simulates daily photosynthesis, the allocation of biomass, crop growth, and development based on four key factors: weather conditions (maximum temperature, minimum temperature, solar radiation, and rainfall), soil characteristics (surface and profile), crop-management practices, and cassava plant genetics (Hoogenboom, Porter, Boote, et al., 2019; Hoogenboom, Porter, Shelia, et al., 2019).

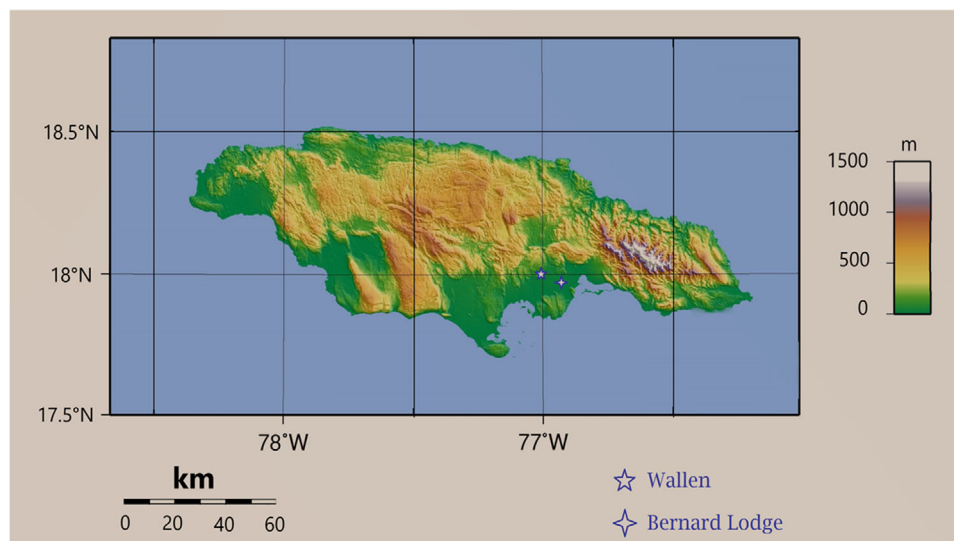


**FIGURE 1** Map of Jamaica showing the location of the Wallen and Bernard Lodge field sites

MANIHOT-Cassava computes daily assimilate as a product of intercepted solar radiation and solar use efficiency. Above-ground growth is prioritized in the model, so partitioning of assimilates is first done to leaves, stems, and fibrous roots. After these demands are met, excess assimilates are sent to storage roots (Moreno-Cadena et al., 2020; Phoncharoen, Banterng, Moreno-Cadena, et al., 2021). The full details of the growth and development processes are described by Moreno-Cadena et al. (2020, 2021). In summary, the node is used as the basic unit of growth for leaves and stems (Moreno-Cadena et al., 2020; Phoncharoen, Banterng, Moreno-Cadena, et al., 2021). The growth rate of nodes depends on the age of the node and the number of leaves when the node appears. Leaf size increases as the crop grows and peaks when the cumulative thermal time reaches 900 degree days ( $^{\circ}\text{Cd}$ ). The accumulation of thermal time also determines other critical processes including forking, as well as the age and growth of leaves. There are no distinct phenological stages and no defined physiological maturity.

## 2.2 | Field experiments

Two experiments were established in St. Catherine, a parish in the southeast of Jamaica (Figure 1), at locations representing different soil and weather conditions. Wallen is located in south-central St. Catherine ( $18^{\circ}10'58''\text{ N}$ ;  $77^{\circ}01'01''\text{ W}$ ), and Bernard Lodge is sited in southeastern St. Catherine ( $17^{\circ}58'58''\text{ N}$ ;  $76^{\circ}52'58''\text{ W}$ ). Four cassava cultivars were planted at each location (BRA 383, CM 849, CM 6119-5, and CM 323-403) and arranged in a randomized complete block design with four replicates at each site (total of 16 plots) per irrigation factor. These cultivars are typically harvested 9–12 mo after planting. At both locations, planting was done

along rows 0.6 m apart with a spacing of 1.5 m between rows. Each plot comprised nine rows and 162 plants in total and had dimensions of 13.7 m (width) by 11.0 m (length). The cropping seasons spanned 19 Dec. 2018 to 15 Nov. 2019 for Wallen and 24 Mar. 2019 to 25 Mar. 2020 at Bernard Lodge.

At Wallen, only rainfed production was undertaken. However, two water treatments (rainfed and irrigated) were investigated at Bernard Lodge (with 16 plots for each irrigation treatment). The irrigation system used surface drippers, and irrigation was done to a depth of 0.3 m and triggered when depletion levels reached about 45% of readily available water (RAW). Fertilization was done twice at each site during the crop season at about 9 and 82 d after planting (DAP). The fertilizer was incorporated into the soil to a depth of 0.1 m. The first application was of NPK blend 14–28–14 (from Newport-Fersan Jamaica Ltd.) equivalent to rates of nitrogen at  $174\text{ kg ha}^{-1}$ , comprised of 40 kg nitrogen as ammonium sulfate and 134 kg nitrogen as diammonium phosphate, phosphorus at  $174\text{ kg ha}^{-1}$  as diammonium phosphate, and potassium at  $140\text{ kg ha}^{-1}$  as potassium chloride. The second application was potassium at  $304\text{ kg ha}^{-1}$  as potassium chloride (from Newport-Fersan Jamaica Ltd).

Several parameters were measured throughout the crop growing season and also at the final harvest. Six plants were tagged in each plot for conducting monthly/bimonthly measurements of plant height, leaf number (by counting nodes with and without leaves), leaf length, and branching characteristics. The measures followed the monitoring recommendations of Ramirez-Villegas et al. (2016). Leaf area was estimated as a function of the mean length of the longest lobe (Lockard et al., 1985; Zanetti et al., 2017) of three leaves per plant tagged. Leaf area index (LAI) was measured using the AccuPAR Linear PAR/LAI Ceptometer (LP-80). The mean of four to six readings taken for each of the tagged plants was



**TABLE 1** Details, irrigation, and climate of the experimental locations at Wallen and Bernard Lodge, St. Catherine parish, Jamaica

Parameter	Wallen	Bernard Lodge
Location	18°10'58" N, 77°01'01" W	17°58'58" N, 76°52'58" W
Elevation, m asl	165	10
Average annual rainfall (1971–2000), mm	1,500–1,750	750–1,000
Cropping season (planting to harvest)	19 Dec. 2018–15 Nov. 2019	24 Mar. 2019–20 Mar. 2020
Cropping season rainfall, mm	1,596.8 <sup>a</sup>	471.8
Cropping season irrigation, mm	–	599 <sup>a</sup>
Cropping season mean $\pm$ SD maximum temperature (range), °C	31.6 $\pm$ 2.0 (24.9–35.4)	33.0 $\pm$ 1.5 (24.7–36.4)
Cropping season mean $\pm$ SD minimum temperature (range), °C	20.6 $\pm$ 1.8 (15.6–24.6)	21.4 $\pm$ 2.1 (15.8–26.8)
Cropping season mean $\pm$ SD solar radiation (range), Wm <sup>-2</sup>	167.5 $\pm$ 42.8 (52.3–271.0)	200.2 $\pm$ 48.0 (35.9–292.54)

<sup>a</sup>Total includes an extreme value of 480 mm received on 1 June 2019. <sup>b</sup>Estimated value.

used for each plot value. The ceptometer measures the above- and below-canopy photosynthetically active radiation (PAR) and calculates LAI based on the ratio of the two. Forking and branching dates were observed and noted when at least 50% of the plants in each plot had branched from the previous level.

For yield and yield components, four plants were randomly sampled from each plot every 2 mo and separated into stems, tubers, and stakes. Care was taken to ensure that the random sampling did not unduly influence competition for light, space, and moisture of the tagged plants. Fresh mass was measured in the field using a Mettler-Toledo Cub BPA224 15-kg digital scale and later oven-dried (at 70 °C) until constant mass to obtain dry mass. The four subsamples were averaged to give a plot value, and the cultivar average was determined from the mean of all four replicates. Total biomass was obtained from the sum of tuber, stems, and stakes. At final harvest, the six tagged plants monitored during the trial were harvested, and similar measurements were taken. Cultivar yield was calculated from the average of four to six plants from each plot and extrapolated to give yield per unit area in kilograms per hectare. Tuber moisture content was inferred from fresh and dry biomass, and harvest index (HI) was calculated as the ratio between tuber mass and total biomass.

### 2.3 | Weather data and soil characteristics

Davis Vantage Pro 2 Automatic weather stations were installed before planting in each location for collecting the weather data. The four variables used for simulation were daily maximum and minimum temperatures, rainfall, and incoming solar radiation. The site at Wallen experienced slightly lower temperatures and less solar radiation than Bernard Lodge (Table 1). Based on the 30-yr (1971–2000) mean annual rainfall analyses by the Meteorological Service,

Jamaica, Bernard Lodge receives up to 750 mm less rainfall than Wallen. Bernard Lodge is warmer and drier, which is typical for locations within the dry coastal fringe of Jamaica's south coast. Irrigation was done only at Bernard Lodge over the period 25 Mar. 2019 to 12 Mar. 2020 and was done to compensate for the lack of rainfall. Because not all the irrigation events were recorded between planting and harvest, we used the automatic irrigation tool available in the model to reflect similar irrigation events to the ones registered in the fieldbook and estimated the irrigation events for the days with missing information. The automated irrigation was based on an allowable depletion threshold of 45% of readily available water and a replenishment point of 100% of RAW. This threshold gave an accumulative irrigation amount of 599 mm (Figure 2).

The soil types differ at the sites. Wallen has (Chudleigh) clay loam soil (Typic Eutrudox), whereas Bernard Lodge has (Dawkins) sandy clay loam (Typic Haplustolls). The initial soil conditions were assessed by collecting soil samples at a depth of 0–0.3 m (Table 2). Based on the values obtained, both sites were deemed to have suitably high micronutrient levels for cassava production except for iron and sulfur (Howeler et al., 2002).

### 2.4 | Model calibration

The CSM-MANIHOT-Cassava model uses 15 cultivar-specific and 15 ecotype parameters. Data from Wallen for the 2018/2019 season and Bernard Lodge 2019/2020 season were used to calibrate the model. Cultivar-specific parameters are adjusted before ecotype parameters. In summary: (a) Sequential adjustments of genetic specific parameters are for forking, from first to fourth forking (parameters: first forking (B01ND), second forking (B12ND), third forking (B23ND), forth forking (B34ND) Steps 1–3 in Phoncharoen, Banterng,

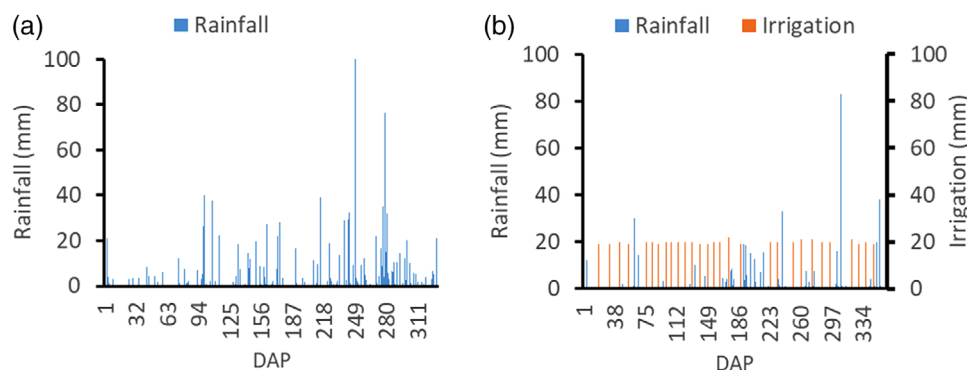


**FIGURE 2** (a) Rainfall at Wallen (cassava growing season December 2018–November 2019). For the sake of comparison, the extreme rainfall value of 480 mm received at 249 d after planting (DAP) is not shown in total but scaled to the maximum axis value of 100 mm. (b) Rainfall and irrigation at Bernard Lodge (cassava crop season March 2019–March 2020)

**TABLE 2** Chemical properties of soils at Wallen (clay loam; Typic Eutrudox) and Bernard Lodge (sandy clay loam; Typic Haplustolls)

Soil chemical property	Wallen	Bernard Lodge
pH	5.1	7.8
Organic matter, %	5.8	2.4
P, mg kg <sup>-1</sup>	3	72
K, mg kg <sup>-1</sup>	57	288
Mg, mg kg <sup>-1</sup>	135	465
Ca, mg kg <sup>-1</sup>	550	1,150
S, mg kg <sup>-1</sup>	40	18
Zn, mg kg <sup>-1</sup>	3.0	3.4
Mn, mg kg <sup>-1</sup>	91	89
Fe, mg kg <sup>-1</sup>	5	4
Cu, mg kg <sup>-1</sup>	2.5	15.2
B, mg kg <sup>-1</sup>	0.3	1.5
CEC, cmol <sub>c</sub> kg <sup>-1</sup>	8.8	20.4
Cation saturation K, %	1.7	3.6
Cation saturation Mg, %	12.8	19.0
Cation saturation Ca, %	31.2	77.3

Note. Mean values for samples taken from a soil depth of 0–0.3 m. CEC, cation exchange capacity.

Moreno-Cadena, et al., 2021); (b) adjustments for leaf number, number of apices, leaf area, LAI, and leaf dry weight (Steps 4–6) (parameters: slope for leaf production (LNSLP), BRnFX, specific leaf lamina area when crop growing without stress (SLAS), leaf life from full expansion to start of senescence [LLIFA], leaf petiole fraction [LPEFR]); (c) adjustments for stem dry weight (Step 7) (parameter: NODWT); (d) adjustments of ecotype parameters for total biomass (Step 8); and (e) check storage root weight and repeat Steps 6 and 7 until acceptable values are obtained (Step 9).

The coefficient of variation was used to show the percentage variation of the parameters between the four cultivars.

The accuracy of the parameters was assessed by comparing simulated with measured values for forking dates, yield and biomass, HI, and LAI. Several statistical indices were used to determine the goodness of fit. These included normalized root mean square error (RMSE<sub>n</sub>) (Equations 1 and 2; Loague & Green, 1991). The RMSE<sub>n</sub> gives a measure (%) of the relative difference of simulated versus observed data. The simulation is considered excellent with a RMSE<sub>n</sub> <10%, good if the RMSE<sub>n</sub> is >10 and <20%, fair if RMSE<sub>n</sub> is >20 and <30%, and poor if the normalized RMSE is >30% (Harb et al., 2016; Jamieson et al., 1991; Soler et al., 2007). In Equation 1,  $P_i$  and  $O_i$  refer to predicted and observed values for the studied variables, respectively (e.g., days from planting to physiological maturity, biomass, yield, and yield components), and  $\bar{o}$  is the mean of the observed variable.

$$\text{RMSE} = \sqrt{\frac{\sum_{i=1}^n \sqrt{(P_i - O_i)^2}}{n}} \quad (1)$$

$$\text{RMSE}_n = \frac{\text{RMSE} \times 100}{\bar{o}} \quad (2)$$

The Index of Agreement ( $d$ ) proposed by Willmott et al. (1985) was estimated using Equation 3. According to the  $d$ -statistic, the closer the index value is to 1, the better the agreement between the two variables that are being compared, and vice versa. In Equation 3,  $n$  is the number of observations,  $P_i$  is the predicted value,  $O_i$  is a measured observation,  $P'i = P_i - \bar{o}$ , and  $O'i = O_i - \bar{o}$ . The coefficient of determination ( $R^2$ ) was also determined.

$$d = 1 - \left( \frac{\sum_{i=1}^n (P_i - O_i)^2}{\sum_{i=1}^n (|P'i| + |O'i|)^2} \right) \quad (3)$$

The percentage deviation (PD) was also calculated to show how closely the end-of-season observed value (at maturity)

matches the simulated by the model. Small deviations are therefore associated with minor differences between end-of-season simulated and measured values (Equation 4). A deviation of zero indicates no difference between simulated and measured values. A positive value means the model is overpredicting the observed value, and a negative value indicates that the model is underpredicting the observed value.

$$PD = \frac{(Pi - Oi) \times 100}{Oi} \quad (4)$$

## 2.5 | Assessing the benefits of irrigation

In this study, two of the higher-yielding cultivars, BRA 383 and CM 849, were used with three irrigation schedules to ascertain the yield response following these conditions:

- Depletion levels: three allowable depletion levels (30, 50, and 75%) of RAW were selected. The automatic irrigation option of the DSSAT beta v4.8 triggered irrigation once this threshold was reached and replenished to a depth of 0.3 m back to 80% of RAW. The depletion and replenishment levels take into consideration the likely availability of water.
- Irrigation method: drip irrigation.
- Assessing response to water: (a) use the simulated yield and biomass as the baseline yield, (b) obtain simulated yield and biomass of the three irrigation treatments and note the cumulative irrigation, (c) compute relative percentage change in yield to ascertain the impact of irrigation and the water use efficiency (WUE), and (d) identify the cultivar response to water and the site at which the most significant benefits are derived.

Water use efficiency was calculated based on yield by dividing the end-of-season tuber dry mass ( $\text{kg ha}^{-1}$ ) by the sum of rainfall and irrigation volume (mm) over the entire season. The relative change approach eliminates the inherent error in the model simulation and assumes the error term of both the baseline and irrigation scenarios are the same. This approach has been used in a number of impact studies (Lallo et al., 2018).

## 3 | RESULTS AND DISCUSSION

### 3.1 | Calibration of the cultivar-specific and ecotype parameters

The value and units of cultivar and ecotype parameters used for the calibration of the model are defined in Table 3. We adjusted 15 cultivar parameters to obtain better agreement between simulated and measured values. By contrast, of the

15 ecotype parameters, only three were adjusted because adjustments of the other parameters did not give better agreement between measured and simulated values. These parameters are PAR conversion factor (PARUE), the PAR extinction coefficient, and harvest product dry matter content. The CV provided a measure of the variation in each parameter between the cultivars.

### 3.2 | Forking characteristics

The duration for each forking level was measured in growing degree days. The cultivar BRA 383, a late-branching variety, had the longest period from planting to first forking (B01ND). The variation between the cultivars for this parameter was small (Table 3). This parameter was reported in previous studies as one of the most critical cultivar parameters (Moreno-Cadena et al., 2020). There was a more significant variation in the duration for first to second forking (B12ND) and third forking (B23ND), as noted by the higher CV. This was primarily driven by the late second branching of BRA 383 but the earlier branching of CM 6119-5 and the comparatively earlier third forking of CM 323-403. The greatest disparity in forking was noted in third to fourth forking (B34ND), as indicated by the large CV of 50.3%. BRA 383 did not have a fourth level of branching, and to account for this, a large thermal time ( $600^\circ\text{Cd}$ ) was used. Phoncharoen et al. (2019) found that days until forking were significantly affected by the environmental conditions at the time of cultivation, including solar radiation, minimum temperature, and day length, with slight genotypic differences in the effect of the conditions on the levels of forking. Considering that the time of planting was similar for all cultivars in this study, the effect of differences in environmental conditions was not a factor, but it could also be that the cultivars have differential responses to photoperiod.

The adjustments made to these parameters resulted in good agreement in forking dates for the cultivars at both sites, with *d*-index values between 0.97 and 0.99. The  $\text{RMSE}_n$  ranged from 4.35 to 14.92% at Wallen and from 7.44 to 15.08% at Bernard Lodge for all varieties. Similar values were reported in calibration for genotypes in Thailand by Phoncharoen, Banterng, Moreno-Cadena, et al. (2021). In general, the model simulated earlier forking at Bernard Lodge for all varieties except the CM 6119-5. This general tendency could have been influenced by the warmer conditions (temperature  $0.8^\circ\text{C}$ ; solar radiation 20% higher) at the site, which would have induced earlier branching that was not fully captured by the model. First forking was delayed in genotypes Rayong 11 and CMR38–125–77 in a study conducted in Thailand when there was less solar radiation ( $16.4 \text{ MJ m}^{-2} \text{ d}^{-1}$ ), a lower minimum temperature ( $23.2^\circ\text{C}$ ), and shorter daylength (12.1 h), but there was no effect in the third genotype Kasetsart 50 (Phoncharoen et al., 2019). At Wallen, the model could not

TABLE 3 Calibrated genetic coefficients for four cassava cultivars (BRA 383, CM 849, CM 6119-5, and CM 323-403) grown at two locations in St. Catherine Parish, Jamaica

Parameter details		Cultivars				
Genetics input file	Genetic parameter	Definition	BRA 383	CM 849	CM 6119-5	CM 323-403
Cultivar						CV %
	B01ND	duration from planting to first forking, °Cd	640	565	530	510
	B12ND	duration from first to second forking, °Cd	260	225	155	210
	B23ND	duration from second to third forking, °Cd	295	228	228	188
	B34ND	duration from third to fourth forking, °Cd	600	200	315	275
	BR1FX	branches per fork at Fork 1, <i>n</i>	2.6	2.5	3.0	2.4
	BR2FX	branches per fork at Fork 2, <i>n</i>	2.8	2.5	3.0	2.4
	BR3FX	branches per fork at Fork 3, <i>n</i>	2.9	2.5	3.0	2.4
	BR4FX	branches per fork at Fork 4, <i>n</i>	2.0	1.0	3.0	2.4
	LAXS	maximum leaf area when growing without stress, cm <sup>2</sup>	583	455	440	505
	SLAS	specific leaf lamina area when crop growing without stress, cm <sup>2</sup> g <sup>-1</sup>	225	210	205	205
	LLIFA	leaf life, from full expansion to start senescence, °Cd	1,260	1,225	1,190	1,205
	LPEFR	leaf petiole fraction (fraction of lamina + petiole)	0.33	0.33	0.33	0.33
	LNSLP	slope for leaf production	1.4	1.5	1.08	1.30
	NODWT	node weight for the main stem before branching at 3,400 °Cd, g	7.90	6.75	8.95	5.89
	NODLT	mean internode length for the main stem before branching when is lignified, cm	4.2	4.1	3.8	4.0
Ecotype						
	PARUE	PAR conversion factor, standard (g dry matter MJ <sup>-1</sup> )	1.60	1.60	1.75	1.56
	KCAN	photosynthetically active radiation extinction coefficient, <i>n</i>	0.59	0.59	0.70	0.56
	HMPC	harvest product dry matter content, %	32	32	30	32
	RSUSE	reserves remobilization fraction (storage roots for tops growth) (fraction)	0.10	0.10	0.10	0.10
	WFSU	water stress factor for leaf senescence (0–1)	0.05	0.05	0.20	0.05



adequately capture the forking characteristics for the varieties. It simulated a later-than-actual forking (by a difference of 3–42 d). The exception was CM 323-403, for which fourth forking was simulated earlier by 18 d than was observed. CM6119-5 presented the greatest challenge at both sites because of its unusual forking pattern, including the short duration of its second forking. Despite several adjustments to B12ND and the other branching parameters, it could not be well simulated.

The number of branches per fork at each forking level, which also affects leaf growth, is defined by four parameters: BR1FX, BR2FX, BR3FX, and BR4FX (defined in Table 3) (Phoncharoen, Banterng, Moreno-Cadena, et al., 2021). The variation between cultivars was small for the first, second, and third forking levels (Table 3). A large variation was noted for the fourth forking level ( $CV = 40\%$ ), representing the marked difference between number of branches at this forking level. Phoncharoen, Banterng, Moreno-Cadena, et al. (2021) reported larger variation in the number of apices for cultivars in Thailand, which differs from the result of this study.

### 3.3 | Leaf growth

Leaf growth is controlled in the MANIHOT-Cassava model by the branching pattern and the following six parameters: maximum leaf area when growing without stress, specific leaf lamina area when crop growing without stress, LLIFA, LPEFR, LNSLP, and PAR extinction coefficient. The variation between these parameters for the four cultivars was small (Table 3). The LPEFR value of 0.33 was defined as default to all varieties and concurred well with observed values obtained in a sensitivity analysis study of model parameters (Moreno-Cadena et al., 2020). The LLIFA did not vary significantly between the cultivars; however, the LNSLP showed greater variation (Table 3). All the cultivars are considered as having medium to high rates of leaf production. The threshold for medium rate is 1.0, and the threshold for high rate is 1.2 (Hoogenboom, Porter, Boote, et al., 2019; Hoogenboom, Porter, Shelia, et al., 2019; Moreno-Cadena et al., 2020). Cassava varieties with high rates of leaf production typically have higher LAI, but long leaf life and leaf area maintenance, especially under moisture stress, strongly promote high root yields (Lahai et al., 1999).

### 3.4 | Stem weight

Stem weight is influenced by mean internode length and node weight. The latter also affects the amount of total biomass partitioned between stem and storage roots (Phoncharoen, Banterng, Moreno-Cadena, et al., 2021). Node weight was also reported as a relevant parameter that affects yields (Moreno-

Cadena et al., 2020). The mean internode lengths were nearly identical for the cultivars, whereas node weight showed more significant variability (Table 3).

## 3.5 | Model evaluation

### 3.5.1 | LAI

The end-of-season values for simulated and measured LAI, biomass, yield, and HI are presented in Table 4. There are small discrepancies between simulated and measured LAI for three of the four cultivars at Wallen, but CM323-403 recorded a high underestimation. At Bernard Lodge, the results were mixed: two cultivars (BRA 383 and CM 849) had a difference of 16% or less, and the other two (CM 6119-5 and CM 323-403) registered high underestimation ( $-39\%$ ). The in-season data (not shown) showed a poor agreement between simulated and measured values. At Wallen, the  $d$ -index was  $<.20$  for three of the four genotypes, and  $RMSE_n$  was  $>29\%$ . At Bernard Lodge, the  $d$ -index value was  $<.50$  for all varieties, and  $RMSE_n$  was  $>57.9\%$ . Several factors could contribute to this poor agreement, including the small number of observed data points (three or less for each site). The model also tended to overpredict initial LAI and showed a near-linear increase in values after 250 DAP. Previous studies (Alves, 2002; Ramirez-Villegas et al., 2016) have reported that when LAI is well simulated, the predictions of biomass and yield are better. Because this relationship is based on yield as storage tubers in cassava, it does not apply equally to all cultivars. CM 6119-5, and to a lesser extent CM 323-403, usually produce excessive shoot growth and fork up to three levels, as noted above. A study aimed at developing a cassava model (Simani-hot) to simulate growth, development, and yield assessed the LAI of five cultivars with different forking patterns and industrial use. Our study found that the simulated values underestimated the LAI in the cultivars that were highly forking and used for forage (Tironi et al., 2017). Because not all the desired measurements of LAI could be conducted during the study, additional data are needed to refine the LAI simulations. This would also improve the simulation of yield because LAI directly affects the growth of storage roots (Phoncharoen, Banterng, Moreno-Cadena, et al., 2021).

### 3.5.2 | Simulation of total biomass

There were small differences between simulated and measured values of end-of-season total biomass at Wallen with a percentage deviation below  $\pm 23\%$  for all cultivars and best results for CM 849 and CM 323-403 (Table 4). Similar deviation values were reported in other studies for the CSM-CERES-Rice Model (Ahmad et al., 2012). The EPIC Model

**TABLE 4** End-of-season observed, simulated, and equivalent percentage deviation for the dry total biomass, yield (dry mass), harvest index (HI), and maximum leaf area index (LAI) for four cassava cultivars at Wallen (harvested 15 Nov. 2019) and Bernard Lodge (harvested 30 Mar. 2020), St. Catherine, Jamaica

Variable	BRA 383	CM 849	CM 6119-5	CM 323-403
Wallen				
Total biomass				
Measured, kg ha <sup>-1</sup>	24,059	16,527	17,241	14,350
Simulated, kg ha <sup>-1</sup>	18,517	18,415	19,423	15,740
Deviation, %	-23.0	11.4	12.7	9.7
Yield				
Measured, kg ha <sup>-1</sup>	13,986 (44,380)	8,760 (23,770)	3,157 (8,649)	8,310 (27,328)
Simulated	9,380 (31,004)	9,723 (32,330)	2,481 (13,646)	7,107 (23,652)
Deviation, %	-32.9 (-30.1)	11.0 (36.0)	-21.4 (57.8)	-14.5 (-13.5)
HI				
Measured	0.58	0.50	0.18	0.58
Simulated	0.51	0.53	0.13	0.45
Deviation, %	-12.1	6.0	-27.8	-22.4
LAI Max				
Measured	3.4	3.5	3.8	2.9
Simulated	3.1	3.0	3.9	2.0
Deviation, %	-8.8	-14.3	-2.6	-31.0
Bernard Lodge				
Total biomass				
Measured, kg ha <sup>-1</sup>	26,032	27,218	30,426	25,383
Simulated, kg ha <sup>-1</sup>	19,649	19,091	16,565	12,915
Deviation, %	-24.5	-29.9	-45.3	-49.1
Yield				
Measured, kg ha <sup>-1</sup>	13,411 (40,111)	14,488 (48,227)	3,401 (15,508)	8,227 (31,716)
Simulated, kg ha <sup>-1</sup>	9,529 (30,927)	10,231 (32,961)	5,640 (12,644)	5,228 (16,962)
Deviation, %	-28.9 (-22.9)	-29.4 (-31.4)	65.8 (-18.5)	-36.5 (-46.5)
HI				
Measured	0.51	0.53	0.19	0.32
Simulated	0.49	0.54	0.20	0.41
Deviation, %	-3.9	1.9	5.3	28.1
LAI Max				
Measured	3.02	2.91	4.9	3.62
Simulated	3.50	2.90	3.00	2.20
Deviation, %	15.9	-0.30	-39.0	-39.2

Note. Values for yield fresh mass are in parentheses

was used to simulate biomass and yield of cassava and other crops species in Cambodia, where there was a strong linear relationship ( $R^2 = .81$ ) between the measured and simulated values for cassava biomass. However, percent deviation between simulated and measured was -27%, exceeding the  $\pm 25\%$  criteria (Le et al., 2018). Adiele et al. (2021) found that there were generally high and significant linear relationships between simulated and measured values for stem growth and root yield in-season and end of season. However, the LIN-

TUL model overestimated the growth in-season under dry conditions. The in-season comparison between simulated and measured biomass is shown in Figure 3a-d, and in-season means and statistical comparisons are given in Table 5. The plots show a fair agreement between simulated and measured biomass for the four cutlivars, and this was confirmed by the high values obtained for  $d$ -index ranging from .94 to .98.

However, using the measured  $RMSE_n$  values of 18.2–38.5%, the simulations would be regarded as fair for only

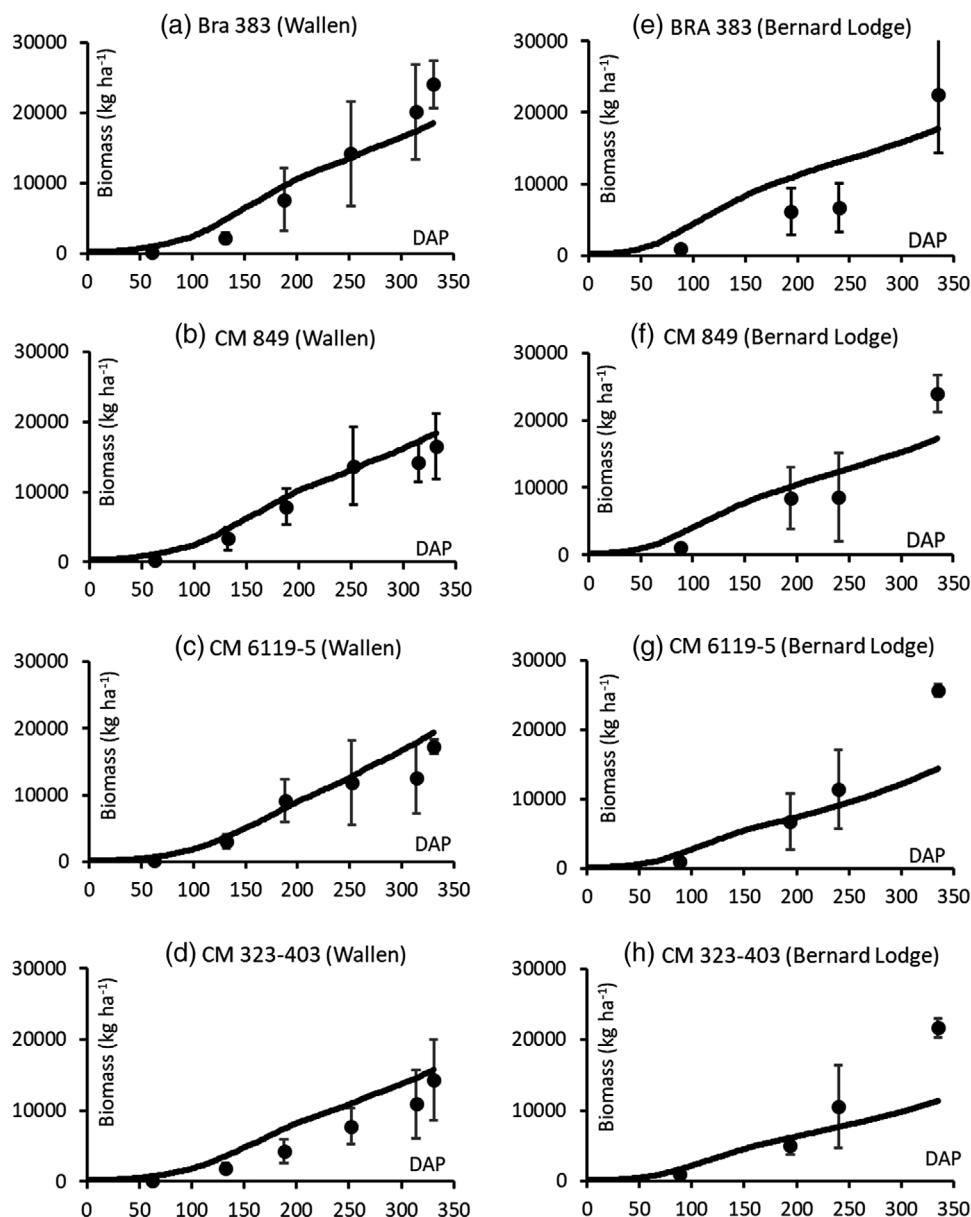


**FIGURE 3** Simulated (line) vs. measured (circle) total biomass at Wallen (a–d) and Bernard Lodge (e–h) plotted against days after planting (DAP) for four cassava cultivars. Wallen was harvested 15 Nov. 2019 and Bernard Lodge on 30 Mar. 2020. Error bars show the 95% confidence interval of measured values

CM 849, and the other cultivars would rank as being poorly simulated. The plots show that much of the discrepancy resulted from the last measurement taken after 300 DAP, which also registered a higher variability. At this location initial conditions were dry resulting in drought stress up to 63 DAP (Figure 2a), but rainfall increased as the season progressed. The model represents well the response of the crop to water availability up to 250 DAP. It is possible that the calibration could be improved by more regular sampling of biomass, as reported by Phoncharoen, Banterng, Moreno-Cadena, et al. (2021). Still, given the distant location and resource constraints, this was not possible in this study.

At Bernard Lodge, crop season rainfall was much lower than that at Wallen, with a difference of over 1,100 mm (Table 1). The warm and dry conditions resulted in higher evapotranspiration levels, poorer sprouting, high drought stress, and ultimate crop failure of all the rainfed plants. The simulation of biomass for the irrigated treatment at Bernard Lodge showed a higher deviation percentage between simulated and measured biomass at the end of the crop season. The model underpredicted the end-of-season biomass for all cultivars (Table 4), but Figure 3e–h shows that the model accounted somewhat better for the in-season biomass. The large deviation exaggerated the differences in mean values for simulated and measured biomass and the values for  $RMSE_n$ .

**TABLE 5** Assessment of simulation of in-season means values of yield (fresh and dry biomass) and total biomass (dry) of four cassava cultivars at Wallen and Bernard Lodge, St, Catherine parish, Jamaica

	Mean		$R^2$	RMSE	Normalized RMSE	$d$ -statistic
Variable	Measured	Simulated				
kg ha <sup>-1</sup>						
Wallen						
BRA 383 total biomass	11,406	10,806	.97	2,887.7	25.3	.96
BRA 383 yield	5,828 (17,872)	4,782 (16,091)	.95 (.91)	2,001.1 (5,511.5)	34.3 (30.8)	.95 (.96)
CM 849 total Biomass	9,316	10,667	.98	1,699.2	18.2	.98
CM 849 yield	4,120 (12,104)	4,810 (16,318)	.98 (.97)	1,144.3 (6,092.7)	27.8 (50.3)	.97 (.92)
CM 6119-5 total biomass	9,014	10,435	.94	2,403.4	26.7	.96
CM 6119-5 yield	1,418 (3,466)	1,978 (7,962)	.46 (.71)	917.0 (5,541.9)	64.7 (159.9)	.74 (.62)
CM 323-403 total biomass	6,568	8,843	.97	2,526.9	38.5	.94
CM 323-403 yield	3,319 (10,478)	3,553 (12,031)	.94 (.90)	798.1 (3,426.5)	24.0 (32.7)	.98 (.97)
Bernard Lodge						
BRA 383 total biomass	12,493	12,958	.85	5,151.9	41.2	.89
BRA 383 yield	5,870 (13,969)	5,919 (17,185)	.76 (.72)	3,000.5 (9,012.0)	51.1 (64.5)	.88 (.89)
CM 849 total biomass	13,842	12,407	.91	5,131.8	37.1	.89
CM 849 yield	6,591 (17,399)	6,000 (17,362)	.84 (.82)	2,946.2 (9,292.7)	44.7 (53.4)	.90 (.90)
CM 6119-5 total biomass	15,075	9,887	.97	8,039.5	53.3	.80
CM 6119-5 yield	2,309 (4,902)	1,913 (6,679)	.88 (.83)	1,320.8 (3,244.2)	57.2 (66.2)	.87 (.92)
CM 323-403 total biomass	12,705	7,944	.95	7,373.7	58.0	.74
CM 323-403 yield	3,966 (1,222)	2,882 (8,262)	.92 (.91)	1,926.6 (7,804.9)	48.6 (63.9)	.86 (.82)

Note. Values are based on the mean of four replicates. Values for fresh mass yield are in parentheses.

confirmed that the simulations were poor (Table 5). Drought stress affects early vegetative growth, which peaks at about 90–180 DAP (Alves, 2002; Ramanujam, 1985). The model properly represents the drought period, but it fails to estimate the recovery phase and final harvest.

Several factors could contribute to the early- and late-season differences between simulated and measured values. These include (a) the model underpredicted the mid-season vegetative growth, (b) differential responses by the cultivars to water stress were observed, and (c) more robust calibration of the coefficients with more than one irrigated treatment is needed to refine the values over different conditions. The CM 6119-5 cultivar deserves special mention because it produced the highest total biomass (30,426 kg ha<sup>-1</sup>) of all the cultivars (second highest at Wallen). However, aboveground biomass accounted for most of the total biomass, and it was very difficult to capture this in the model without adversely affecting yield simulation. Because CM 6119-5 produces significant branching and shoot mass, it could be recommended for animal feed.

Valuable lessons were learned from the crop failure of the rainfed treatment at Bernard Lodge that emphasize the impor-

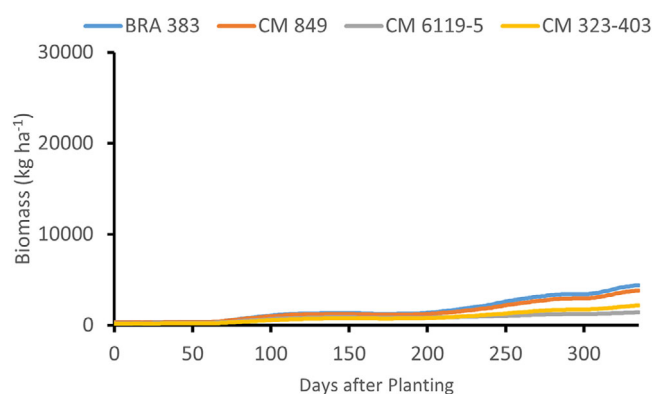


**FIGURE 4** Simulated biomass at Bernard Lodge, St Catherine parish, Jamaica for four rainfed cassava cultivars

tance of irrigation to agricultural production within the dry coastal fringe of Jamaica. The model captured the crop failure of the rainfed trial (Figure 4). In every case, the simulated biomass was <5,000 kg ha<sup>-1</sup>, although the order of the cultivars was slightly reversed relative to the irrigated treatment, with CM 6119-5 being the least productive genotype. This

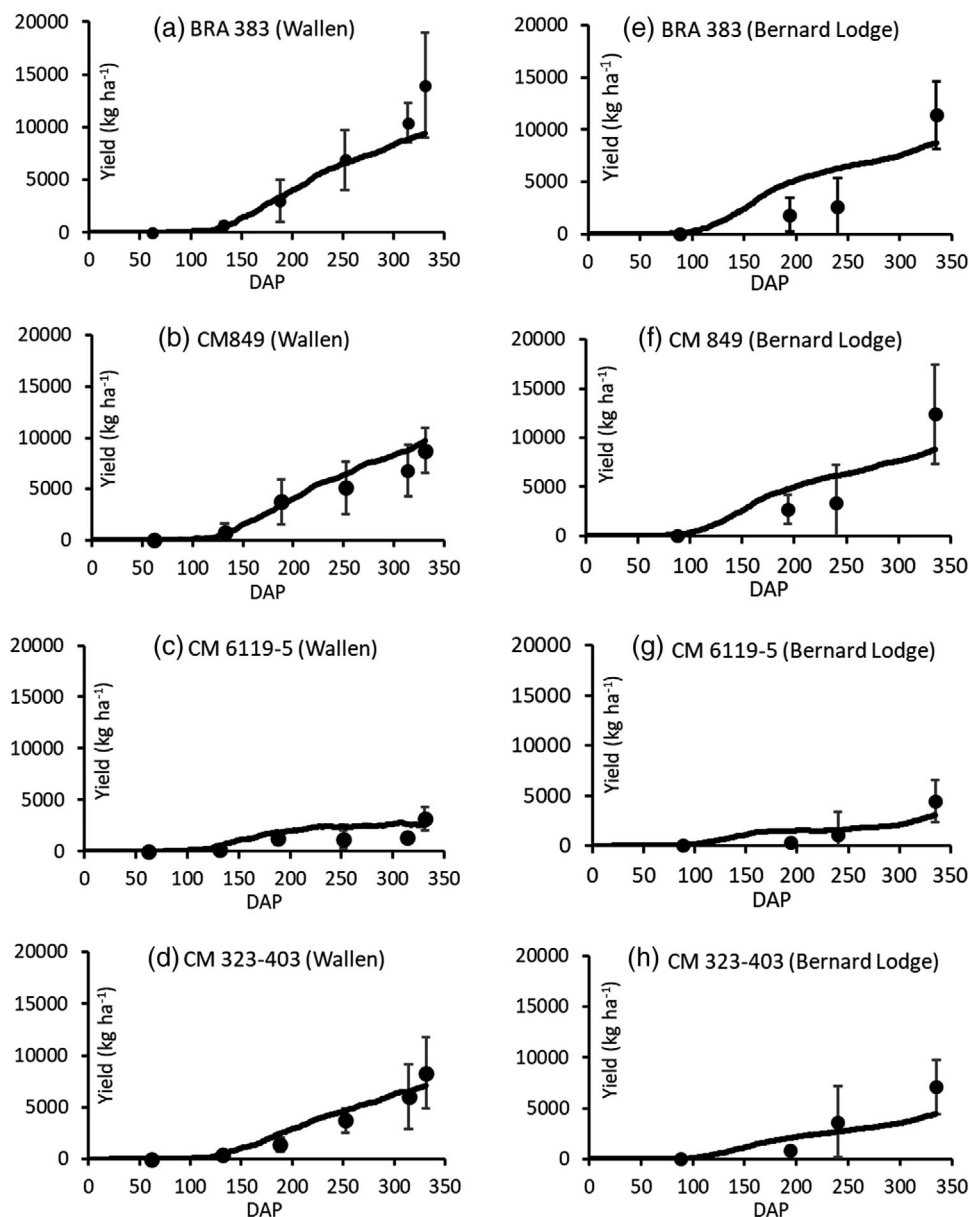


**FIGURE 5** Measured (circle) vs simulated (line) yield (dry mass) at Wallen (a–d) and Bernard Lodge (e–h) for four cassava cultivars. Wallen was harvested on 15 Nov. 2019 and Bernard Lodge on 30 Mar. 2020. Error bars show the 95% confidence interval of measured values. DAP, days after planting

finding is helpful in that it presents an opportunity to explore both the limits of cassava's drought tolerance and proactively identify critical thresholds for viable production under irrigation.

### 3.6 | Simulation of yield and HI

#### 3.6.1 | Yield

Based on dry biomass, the end-of-season yield at Wallen did not give quite as good agreement of simulated and observed values as for biomass for CM 6119-5 and considerably worse

agreement for Bra 383 (Table 4). Nevertheless, the plots in Figure 5a–d show that the in-season simulation up to 250 DAP had a good agreement between measured and simulated values for three of the four genotypes ( $d = .94-.97$ ). However, the  $RMSE_n$  values ranged from 24.0 to 64.7%, and only two cultivars (CM 849 and CM 323-403) had a fair simulation (Table 5).

One new feature of the DSSAT beta v4.8 CSM-MANIHOT model is its ability to simulate yield based on fresh biomass. This added feature provides an opportunity to explore the prediction of yield without having to dry samples. Based on fresh biomass, the deviations were higher ( $-13.5$  to  $+57.8\%$ ) and  $d$ -index values were largely unchanged, but  $RMSE_n$  values were



much higher (32.7–159.9), suggesting that it may be more difficult to predict yield based on fresh weight.

The failure to predict fresh biomass could be due to the differential moisture content of the varieties and factors, like the proportion of leaves to stem of shoots. The discrepancies between simulated and measured yield highlight challenges associated with obtaining accurate simulation of cassava yields and are similar to those reported in previous cassava modeling studies (Gabriel et al., 2014; Phoncharoen, Banterng, Moreno-Cadena, et al., 2021; Ramirez-Villegas et al., 2016). Yield prediction of root crops (like cassava and sweet potato) tends to be more challenging because of several factors, including the nonlinear development of tubers and differences in cultivar responses to the same local field conditions (Fielding & Ryder, 1995; Lebot, 2009; Martin & Carmer, 1985). More frequent sampling could improve the simulations, and this requires large field plots and more resources to carry out all necessary measurements.

Data were only available for one rainfed trial because of the failure of the rainfed crop at Bernard Lodge. Under these circumstances, it was difficult to obtain parameters that adequately suited both the rainfed conditions at Wallen and the irrigated trial at Bernard Lodge. At Bernard Lodge, the model underpredicted end-of-season dry and fresh yield by at least 23% for almost all the cultivars. The exception was CM6119-5, which recorded an overprediction of 65.8% for yield dry mass but an underprediction of 18.5% for yield fresh mass (Table 4). This variety was particularly challenging given that most of its biomass is apportioned to stems and leaves, which could not be accurately captured by model parameters for both sites. At Bernard Lodge, the values of the *d*-index for yield were virtually the same when reckoned by both fresh and dry yield with values  $>.82$ . The RMSE<sub>n</sub> values were above 45%, suggesting simulations were poor and higher for fresh than dry yield. The plot of yield (dry biomass) in Figure 5e–h shows that the most significant disparity in measured and simulated occurred at the end of the season. The model was able to simulate the failure of the rainfed treatment, and all the cultivars recorded yields of  $<400 \text{ kg ha}^{-1}$  with a lowest of  $9 \text{ kg ha}^{-1}$  for CM 6119-5 (data not shown). This further affirms that the model can be used to investigate the impacts of drought on cassava production. From the experimental results, three of the four cultivars (BRA 383, CM 849, and CM232-403) are higher yielding and are more tolerant to water stress when compared to CM 6119-5.

### 3.6.2 | HI

Harvest index measures the proportion of total biomass accounted by the economic portion of the crop, in this case, the storage roots. It usually reflects the correlation that commonly occurs between total biomass and yield (Ramanujam,

1990; Alvez, 2002; Moreno-Cadena et al., 2020, 2021; Phoncharoen, Banterng, Moreno-Cadena, et al., 2021). The model predicted the end-of-season HI at both sites, with deviation percentages ranging from  $-27.8$  to  $+28.1\%$ . An underprediction (of  $-27.8\%$ ) was noted at Wallen for CM 6119-5, but a slight overestimation of  $5.3\%$  was noted at Bernard Lodge (Table 4).

### 3.6.3 | The benefits of irrigation: Insights into future water demand

The cultivars BRA 383 and CM 849 have consistently recorded higher yields at both sites than the CM 6119-5 and CM 323-403. We investigated the yield response to three irrigation scenarios at each location. The irrigation depletion thresholds used were 30% (Auto 30), 50% (Auto 50), and 75% (Auto 75) of RAW, a management irrigation depth of 0.3 m, and a replenishment endpoint of 80% of RAW. The higher the allowable threshold, the faster the irrigation will be triggered and the higher the irrigation amount will be.

Table 6 summarizes the results of the simulations and includes estimates of WUE. The increased supply of water results in increased yields at both sites, but the changes for both yield and WUE depended on the amount of irrigation and cultivar (Table 6). The irrigation required by each cultivar was nearly identical at each replenishment rate. At Wallen the irrigation requirements are up to five times less compared with Bernard Lodge due to the difference in rainfall, with Bernard Lodge receiving about 1,100 mm less than Wallen (Table 1). At Wallen, an increase in yield with irrigation was modest for all treatments, but CM 849 was predicted to benefit (17% increase in yield for a depletion threshold of 50% of RAW) slightly more than Bra 383 (11% corresponding increase). The WUE showed an optimal response, reaching a maximum for both cultivars when the depletion threshold is 50% of RAW, but increases in efficiency were small compared with the rainfed baseline: 3% for BRA 383 and 8% for CM 849. This suggests that the beneficial effects of irrigation might not outweigh the costs of irrigation at Wallen. As noted above, crops are not productive without irrigation at Bernard Lodge. Yield increased linearly with higher irrigation for both cultivars at this location, and again CM 849 was marginally more responsive to water. The response of WUE to all the irrigation treatments was higher than at Wallen by 30–40% for both cultivars. However, the optimum was similar and occurred when the depletion threshold for irrigation was around 45% of RAW.

## 4 | KEY CONSIDERATIONS

The experience with this study has generated important lessons, and key considerations are the following.

**TABLE 6** Simulated yield response to irrigation relative to rainfed simulations for cassava cultivars BRA 383 and CM 849 at Wallen and Bernard Lodge, St. Catherine Parish, Jamaica

Site/irrigation treatment		Yield		Irrigation amount		Relative yield increase		Water use efficiency <sup>a</sup>	
		kg ha <sup>-1</sup>		mm		% of baseline		kg ha <sup>-1</sup> mm <sup>-1</sup>	
Site	Irrigation treatment	BRA 383	CM 849	BRA 383	CM 849	BRA 383	CM 849	BRA 383	CM 849
Wallen	0	9,380	9,723	0	0	0	0	5.9	6.1
	Auto 30	10,132	10,973	95	94	8	13	6.0	6.5
	Auto 50	10,458	11,363	130	129	11	17	6.1	6.6
	Auto 75	10,054	11,503	209	209	7	18	5.6	6.4
Bernard Lodge	0	499	279	0	0	0	0	1.1	0.6
	Auto 30	7,940	7,886	492	474	1,491	2,727	8.2	8.3
	Auto 45 <sup>a</sup>	9,529	10,231	599	599	1,810	3,567	8.9	9.6
	Auto 50	9,726	10,583	716	740	1,849	3,693	8.2	8.7
	Auto 75	10,584	11,412	882	908	2,021	3,990	7.8	8.3

Note. Auto 30, Auto 50, and Auto 75 represent an allowable depletion of readily available water (RAW) of 30, 50, and 75%, respectively; replenishment end point was 80% of RAW. Water use efficiency is based on yield (using dry mass).

<sup>a</sup>Using total volume of water as the sum of irrigation and rainfall; rainfall was 1597 mm for Wallen, 472 mm for Bernard Lodge. <sup>b</sup>Replenishment endpoint was 75% RAW for this treatment.

#### 4.1 | CSM-MANIHOT-Cassava model

The calibration of the model requires detailed field experiments and would best be done with at least two seasons worth of data with sufficient replicates to test the parameters rigorously. Although many challenges were encountered, the results are promising and have provided key insights into essential production thresholds. The ability to explore multiple scenarios, test several cultivars, and simulate using fresh biomass are advantages that should spur interest in future work.

#### 4.2 | Challenges and opportunities

The resource constraints of small island developing states and the lack of field stations require collaboration with external agencies to conduct scientific research. Lack of resources restricts the frequency with which data can be collected and the number of parameters that can be adequately monitored, especially for distant locations. This, in turn, affects the quality of modeling work and the applicability of results. On the other hand, it provides opportunities for collaboration with multiple stakeholders to leverage resources and increase ownership.

#### 4.3 | Key inferences

The difference in environmental conditions at the two sites proved very challenging, and it was difficult to find a set of parameters that adequately suited the conditions at both

sites. It was not possible to evaluate the rigor of the parameters with an independent data set. This suggests that further work is needed to sufficiently refine the parameters and test their robustness over a wide set of environmental conditions. Notwithstanding, a number of inferences can be made: (a) the CSM-MANIHOT-Cassava model can be calibrated for locally grown cultivars; (b) the in-season simulation was good for both yield and biomass, suggesting that, even with limited data, the growth and development of cassava can be tracked; (c) the ability of the model to simulate the crop failure at Bernard Lodge was instrumental, suggesting that the model can be used as a critical planning tool to explore a number of “what if” scenarios before costly investments are made in agricultural production; (d) the investigation of the benefits of irrigation demonstrates that yield responses vary between cultivars in the same environment and suggests that irrigation will become increasingly important as the Caribbean region becomes warmer and drier (as projected by climate models); and (e) the model can be used to prioritize adaptation options to cope with the known and anticipated adverse impacts of climate variability and change. Among options that should be explored are identifying heat- and drought-tolerant genotypes to improve food security and reduce reliance on imported foods.

## 5 | CONCLUSION

The study calibrated four cassava cultivars in the CSM-MANIHOT cassava model in DSSAT beta v4.8. The two field experiments allowed the testing of rainfed and irrigated conditions in the model, and reasonably good simulations of

in-season yield, biomass, and HI were obtained for most cultivars. However, end-of-season yield was less well simulated, especially for the irrigated site. The simulation of LAI was particularly challenging but was affected by the limited data, so improvements to LAI calibration could increase the robustness of the parameters. The clear benefits of irrigation to production at Bernard Lodge emphasize the importance of irrigation in a warmer Caribbean under climate change. Although further work is needed to refine the parameters, progress has been made in adding new cultivars and experiments to the DSSAT cassava experiments. The study results should help pique interest in the region pursuing modeling as a climate change adaptation tool.

## ACKNOWLEDGMENTS

This Project was funded by the Adaptation Programme and Financing Mechanism for the Pilot Programme for Climate Resilience under its Special Climate Change Adaptation Fund administered by the Environmental Foundation of Jamaica. We also gratefully acknowledge assistance from the Caribbean Regional Track of the Pilot Programme for Climate Resilience funded by the Inter-American Development Bank (IDB); Desnoes and Geddes Foundation and IDB Project Grow: Accelerating the Inclusion of Small Scale Farmers and Youth Into the Commercial Cassava Value Chain; Red Stripe, part of the Heineken Company; the Meteorological Service of Jamaica, and the Decision Support System for Agro-technology Transfer Foundation.

## AUTHOR CONTRIBUTIONS

Dale Rankine: Conceptualization; Formal analysis; Funding acquisition; Investigation; Methodology; Validation; Writing-original draft; Writing-review & editing. Jane E. Cohen: Conceptualization; Data curation; Formal analysis; Funding acquisition; Investigation; Methodology; Project administration; Supervision; Validation; Writing-review & editing. Fradian V.N. Murray: Data curation; Formal analysis; Methodology; Writing-review & editing. Patricia Moreno-Cadena: Methodology; Software; Validation; Writing-review & editing. Gerrit Hoogenboom: Methodology; Software; Supervision; Writing-review & editing. Jayaka D. Campbell: Conceptualization; Data curation; Software; Visualization. Michael A. Taylor: Funding acquisition; Resources; Supervision; Writing-review & editing. Tannecia Stephenson: Funding acquisition; Resources; Supervision; Writing-review & editing.


## CONFLICT OF INTEREST

The authors declare no conflict of interest.

## ORCID

Dale Rankine  <https://orcid.org/0000-0001-9227-9368>

Jane Cohen  <https://orcid.org/0000-0003-4933-6106>

Patricia Moreno-Cadena  <https://orcid.org/0000-0002-8326-6124>

Gerrit Hoogenboom  <https://orcid.org/0000-0002-1555-0537>

## REFERENCES

- Adiele, J. G., Schut, A. G. T., van den Beuken, R. P. M., Ezui, K. S., Pypers, P., Ano, A. O., Egesi, C. N., & Giller, K. E. (2021). A recalibrated and tested LINTUL-Cassava simulation model provides insight into the high yield potential of cassava under rainfed conditions. *European Journal of Agronomy*, 124, 1–12. <https://doi.org/10.1016/j.eja.2021.126242>
- Ahmad, S., Ahmad, A., Soler, C. M. T., Ali, H., Zia-Ul-Haq, M., Anothai, J., Hussain, A., Hoogenboom, G., & Hasanuzzaman, M. (2012). Application of the CSM-CERES-Rice model for evaluation of plant density and nitrogen management of fine transplanted rice for an irrigated semiarid environment. *Precision Agriculture*, 13, 200–218. <https://doi.org/10.1007/s11119-011-9238-1>
- Alves, A. A. C. (2002). Cassava botany and physiology. In R. J. Hillocks, J. M. Thresh, & A. C. Bellotti (Eds.), *Cassava: Biology, production and utilization* (pp. 67–90). CAB International.
- Ayling, S., Ferguson, M., Rounsley, S., & Kulakow, P. (2012). Information resources for cassava research and breeding. *Tropical Plant Biology*, 5, 140–151. <https://doi.org/10.1007/s12042-012-9093-x>
- Brockamp, K. (2016). Postharvest loss in the Caribbean. *i-ACES*, 2, 37–43.
- CIAT. (2011). *The Cassava handbook: A reference manual based on the Asian Regional Cassava Training Course held in Thailand*. CIAT.
- Climate Studies Group Mona (CSGM). (2012). *State of the Jamaican climate 2012: Information for resilience building (full report)*. Planning Institute of Jamaica.
- Climate Studies Group Mona (CSGM). (2017). *State of the Jamaican climate 2015: Information for resilience building (full report)*. Planning Institute of Jamaica.
- El-Sharkaway, M. A. (2004). Cassava biology and physiology. *Plant Molecular Biology*, 56, 481–501. <https://doi.org/10.1007/s11103-005-2270-7>
- Ezui, K., Leffelaar, P., Franke, A., Mando, A., & Giller, K. (2018). Simulating drought impact and mitigation in cassava using the LINTUL model. *Field Crops Research*, 219, 256–272. <https://doi.org/10.1016/j.fcr.2018.01.033>
- FAO. (2013a). Water management. In *Save and grow: Cassava, A guide to sustainable production intensification*. FAO.
- FAO. (2013b). *CARICOM food import bill, food security and nutrition* (Issue Brief #5). Subregional Office for the Caribbean.
- FAO. (2015). *FAO working to reduce post-harvest food loss in CARICOM*. FAO Regional Office for Latin America and the Caribbean. <http://www.fao.org/americas/noticias/ver/en/c/328019/>
- FAO. (2020). *OECD-FAO agricultural outlook 2020-2029*. FAO.
- Fielding, W., & Ryder, R. (1995). *The biometry of sweet potato (Ipomoea batatas): Some considerations for field experiments* (Special Publication No. 8). Ministry of Agriculture and Mining.
- Gabriel, L. F., Streck, N. A., Roberti, D. R., Chielle, Z. G., Uhlmann, L. O., da Silva, M. R., & da Silva, S. D. (2014). Simulating cassava growth and yield under potential conditions in Southern Brazil. *Agronomy Journal*, 106, 1119–1137. <https://doi.org/10.2134/agronj2013.0187>

- Gijzen, H., Veltkamp, H. J., Goudriaan, J., & Bruijn, G. D. (1990). Simulation of dry matter production and distribution in cassava (*Manihot esculenta* Crantz). *Netherlands Journal of Agricultural Science*, 38, 159–173.
- Harb, O. M., Abd El-Hay, G. H., Hager, M. A., & Abou El-Enin, M. M. (2016). Calibration and validation of DSSAT V.4.6.1, CERES and CROPGRO models for simulating no-tillage in Central Delta, Egypt. *Agrotechnology*, 5, 1–9. <https://doi.org/10.4172/2168-9881.1000143>
- Hoogenboom, G. K. J., Boote, K. J., Porter, C. H., Singh, U., & Batchelor, W. D. (2018). *Modular summer training in the DSSAT application software*. University of the West Indies.
- Hoogenboom, G., Porter, C. H., Boote, K. J., Shelia, V., Wilkens, P. W., Singh, U., White, J. W., Asseng, S., Lizaso, J. I., Moreno, L. P., Pavan, W., Ogoshi, R., Hunt, L. A., Tsuji, G. Y., & Jones, J. W. (2019). The DSSAT crop modeling ecosystem. In K. J. Boote (Ed.), *Advances in crop modeling for a sustainable agriculture* (pp. 173–216). Burleigh Dodds Science Publishing.
- Hoogenboom, G., Porter, C. H., Shelia, V., Boote, K. J., Singh, U., White, L. A., Hunt, L. A., Ogoshi, R., Lizaso, J. I., Koo, J., Asseng, S., Singles, A., Moreno, L. P., & Jones, J. W. (2019). *Decision Support System for Agrotechnology Transfer (DSSAT) Version 4.7.5*. DSSAT Foundation.
- Hoogenboom, G., Porter, C. H., Shelia, V., Boote, K. J., Singh, U., White, J. W., Pavan, W., & Jones, J. W. (2021). *Decision Support System for Agrotechnology Transfer (DSSAT) Version 4.8 beta*. DSSAT Foundation.
- Howeler, R. (2002). Mineral nutrition. In R. J. Hillocks & J. M. Thresh (Eds.), *Cassava biology, production and utilization* (pp. 115–147). CAB International.
- Hunt, L. A., & Boote, K. J. (1998). Data for model operation, calibration and evaluation. In G. Y. Tsuji, G. Hoogenboom, & P. K. Thornton (Eds.), *Understanding options for agricultural production* (pp. 9–39). Kluwer Academic Publishers.
- Isaiah, A. I., Yamusa, A., & Odunze, A. C. (2020). Impact of climate change on rainfall distribution on cassava yield in coastal and upland areas of Akwa Ibom State, Nigeria. *Journal of Experimental Agriculture International*, 42, 44–53.
- Jamieson, P. D., Porter, J. R., & Wilson, D. R. (1991). A test of the computer simulation model ARC-WHEAT1 on wheat crops grown in New Zealand. *Field Crops Research*, 27, 337–350. [https://doi.org/10.1016/0378-4290\(91\)90040-3](https://doi.org/10.1016/0378-4290(91)90040-3)
- Jones, J. W., Hoogenboom, G., Porter, C. H., Boote, K. J., Batchelor, W. D., Hunt, L. A., Wilkens, P. W., Singh, U., Gijsman, A. J., & Ritchie, J. T. (2003). DSSAT cropping system model. *European Journal of Agronomy*, 18, 235–265. [https://doi.org/10.1016/S1161-0301\(02\)00107-7](https://doi.org/10.1016/S1161-0301(02)00107-7)
- Lahai, M. T., George, J. B., & Ekanayake, I. J. (1999). Cassava (*Manihot esculenta* Crantz) growth indices, root yield and its components in upland and inland valley ecologies of Sierra Leone. *Journal of Agronomy & Crop Science*, 182, 128–136. <https://doi.org/10.1046/j.1439-037x.1999.00299.x>
- Lallo, C. H. O., Cohen, J., Rankine, D., Taylor, M., Cambell, J., & Stephenson, T. (2018). Characterizing heat stress on livestock using the temperature humidity index (THI): Prospects for a warmer Caribbean. *Regional Environmental Change*, 18, 2329–2340. <https://doi.org/10.1007/s10113-018-1359-x>
- Le, K. N., Jeong, J., Reyes, M. R., Jha, M. K., Gassman, P. W., Doro, L., Hok, L., & Boulakia, S. (2018). Evaluation of the performance of the EPIC model for yield and biomass simulation under conservation systems in Cambodia. *Agricultural Systems*, 166, 90–100. <https://doi.org/10.1016/j.agsy.2018.08.003>
- Lebot, V. (2009). *Tropical root and tuber crops: Cassava, sweet potato, yams and aroids*. CAB International.
- Loague, K., & Green, R. E. (1991). Statistical and graphical methods for evaluating solute transport models: Overview and application. *Journal of Contaminant Hydrology*, 7, 51–73. [https://doi.org/10.1016/0169-7722\(91\)90038-3](https://doi.org/10.1016/0169-7722(91)90038-3)
- Lockard, R. G., Lockard, J. M., & Wounuah, D. D. (1985). A rapid non-destructive method for the estimation of leaf areas in cassava. *Annals of Botany*, 55, 125–128.
- Martin, F. W., & Carmer, S. G. (1985). Variations in sweet potato for tolerance to some physical and biological stresses. *Euphytica*, 34, 457–466. <https://doi.org/10.1007/BF00022942>
- Matthews, R. B., & Hunt, L. A. (1994). GUMCAS: A model describing the growth of cassava (*Manihot esculenta* L. Crantz). *Field Crops Research*, 36, 69–84. [https://doi.org/10.1016/0378-4290\(94\)90054-X](https://doi.org/10.1016/0378-4290(94)90054-X)
- Moreno-Cadena, L. P. (2018). Modelo de simulación de yuca (*Manihot esculenta* Crantz) en el trópico [Master's thesis]. Universidad Nacional de Colombia.
- Moreno-Cadena, L. P., Hoogenboom, G., Fisher, M. J., Ramirez-Villegas, J., Prager, S. P., Lopez-Lavalle, L. A. B., Pypers, P., Mejia de Tafur, M. S., Wallach, D., Munoz-Carpena, R., & Asseng, S. (2020). Importance of genetic parameters and uncertainty of MANIHOT, a new mechanistic cassava simulation model. *European Journal of Agronomy*, 115, 1–14. <https://doi.org/10.1016/j.eja.2020.126031>
- Moreno-Cadena, P., Hoogenboom, G., Cock, J. H., Ramirez-Villegas, J., Pypers, P., Kreye, C., Tariku, M., Ezui, K. S., Lopez-Lavalle, L. A. B., & Asseng, S. (2021). Modeling growth, development and yield of cassava: A review. *Field Crops Research*, 267, 1–13. <https://doi.org/10.1016/j.fcr.2021.108140>
- Mtunduja, M. K., Thitisaksakul, M., Muzanila, Y. C., Wansuksri, R., Piyachomkwan, K., Laswai, H. S., & Beckles, D. M. (2016). Assessing variation in physicochemical, structural, and functional properties of root starches from novel Tanzanian cassava (*Manihot esculenta* Crantz.) landraces. *Stärke*, 68, 1–14. <https://doi.org/10.1002/star.20150017>
- Penning de Vries, F. W., & van Laar, H. H. (Eds.). (1982). *Simulation of plant growth and crop production*. Wageningen: Simulation monographs. Pudoc.
- Phoncharoen, P., Banterng, P., Vorasoot, N., Jogloy, S., Theerakulpisut, P., & Hoogenboom, G. (2019). The impact of seasonal environments in a tropical savanna climate on forking, leaf area index, and biomass of cassava genotypes. *Agronomy*, 9, 19. <https://doi.org/10.3390/agronomy9010019>
- Phoncharoen, P., Banterng, P., Moreno-Cadena, L. P., Vorasoot, N., Jogloy, S., Theerakulpisut, P., & Hoogenboom, G. (2021). Performance of the CSM-MANIHOT-Cassava model for simulating planting date response of cassava genotypes. *Field Crop Research*, 264. <https://doi.org/10.1016/j.fcr.2021.108073>
- Phoncharoen, P., Banterng, P., Vorasoot, N., Jogloy, S., Theerakulpisut, P., & Hoogenboom, G. (2021). Identifying suitable genotypes for different cassava production environments: A modeling approach. *Agronomy*, 11, 1372. <https://doi.org/10.3390/agronomy11071372>
- Prochnik, S., Marri, P. R., Desany, B., Rabinowicz, P. D., Kodira, C., Mohiuddin, M., Rodriguez, F., Fauquet, C., Tohme, J., Harkins, T., Rokhsar, D. S., & Rounsley, S. (2012). The Cassava genome: Current progress, future directions. *Tropical Plant Biology*, 5, 88–94. <https://doi.org/10.1007/s12042-011-9088-z>



- Ramanujam, T. (1985). Leaf density profile and efficiency in partitioning dry matter among high and low yielding cultivars of cassava (*Manihot esculenta* Crantz). *Field Crops Research*, 10, 291–303.
- Ramanujam, T. (1990). Effect of moisture stress on photosynthesis and productivity of cassava. *Photosynthetica*, 24, 217–224.
- Ramirez-Villegas, J., Soto, J. S., Amariles, D. A., Moreno, P., Aye, T. M., Fisher, M., & Cock, J. (2016). *Towards an improved cassava simulation model to aid management decisions in the tropics*. CIAT, Hung Loc Agricultural Research Centre and Soils and Fertilizers Research Institute.
- Reincke, K., Vilvert, E., Fasse, A., Graef, F., Sieber, S., & Lana, M. A. (2018). Key factors influencing food security of smallholder farmers in Tanzania and the role of cassava as a strategic crop. *Food Security*, 10, 911–924. <https://doi.org/10.1007/s12571-018-0814-3>
- Robin, G. C., Asiedu, F. Lopez, V., & Extavour, V. (2018). Roots and tubers research and development activities in countries of the Caribbean community with a focus on cassava (*Manihot esculenta* Crantz). *Universal Journal of Agricultural Research*, 6, 214–230. <https://doi.org/10.13189/ujar.2018.060604>
- Scott, G. J. (2021). A review of root, tuber and banana crops in developing countries: Past, present and future. *International Journal of Food Science & Technology*, 56, 1093–1114. <https://doi.org/10.1111/ijfs.14778>
- Soler, C. M. T., Sentelhas, P. C., & Hoogenboom, G. (2007). Application of the CSM-CERES-Maize model for planting date evaluation and yield forecasting for maize grown off-season in a subtropical environment. *European Journal of Agronomy*, 27, 165–177. <https://doi.org/10.1016/j.eja.2007.03.002>
- Stephenson, T. S., Vincent, L. A., Allen, T., Van Meerbeeck, C. J., McLean, N., Peterson, T. C., Taylor, M. A., Aaron-Morrison, A. P., Auguste, T., Bernard, D., Boekhoudt, J. R. I., Blenman, R. C., Braithwaite, G. C., Brown Glenroy, B., Butler, M., Cumberbatch, C. J. M., Etienne-Leblanc, S., Lake, D. E., Martin, D. E., ..., & Trotman, A. R. (2014). Changes in extreme temperature and precipitation in the Caribbean region, 1961–2010. *International Journal of Climatology*, 34(9), 2957–2971. <https://doi.org/10.1002/joc.3889>
- Tironi, L. F., Streck, N. A., Gubiani, P. I., Benedetti, R. P., & De Freitas, C. P. d. O. (2017). Simanihot: A process-based model for simulating growth, development and productivity of cassava. *Journal of the Brazilian Association of Agricultural Engineering*, 37, 471–83. <https://doi.org/10.1590/1809-4430-Eng.Agric.v37n3p471-483/2017>
- Tonukari, N. J. (2004). Cassava and the future of starch. *Electronic Journal of Biotechnology*, 7, 5–8.
- Tsuji, G. Y., Hoogenboom, G., & Thornton, P. K. (1998). *Understanding options for agricultural production. Systems approaches for sustainable agricultural development*. Kluwer Academic Publishers.
- Willmott, C. J., Akleson, G. S., Davis, R. E., Feddema, J. J., Klink, K. M., Legates, D. R., Odonnell, J., & Rowe, C. M. (1985). Statistics for the evaluation and comparison of models. *Journal of Geophysical Research*, 90, 8995–9005. <https://doi.org/10.1029/JC090iC05p08995>
- Veltkamp, H. (1986). *Physiological Causes of Yield Variation in Cassava (Manihot esculenta Crantz)*. [Doctoral dissertation Wageningen Agricultural University]. <https://edepot.wur.nl/205651>
- Zanetti, S., Pereira, L. F. M., Sartori, M. M. P., & Silva, M. A. (2017). Leaf area estimation of cassava from linear dimensions. *Anais da Academia Brasileira de Ciencias*, 89, 1729–1736. <https://doi.org/10.1590/0001-376520172016-0475>

**How to cite this article:** Rankine, D., Cohen, J., Murray, F., Moreno-Cadena, P., Hoogenboom, G., Campbell, J., Taylor, M., & Stephenson, T. Evaluation of DSSAT-MANIHOT-Cassava model to determine potential irrigation benefits for cassava in Jamaica. *Agronomy Journal*. 2021;113:5317–5334. <https://doi.org/10.1002/agj2.20876>